6th European Conference on Computational Mechanics (ECCM 6)
7th European Conference on Computational Fluid Dynamics (ECFD 7)
11 – 15 June 2018, Glasgow, UK

INFLUENCE OF THE WIND TURBULENCE ON THE STANDARD AND COUNTER-ROTATING VAWT PERFORMANCES

HORIA DUMITRESCU[1], ALEXANDRU DUMITRACHE[1], ION MALAEL[2] AND RADU BOGATEANU[3]

[1] "Gh. Mihoc-C. Iacob"Institute of Mathematical Statistics and Applied Mathematics
Calea 13Septembrie 13, 013968 Bucharest, Romania
dumitrescu.horia@yahoo.com, alex_dumitrache@yahoo.com

[2] National Research and Development Institute for Gas Turbine, COMOTI
B-dul Iuliu Maniu 220, 061126 Bucharest, Romania
ion.malael@comoti.ro

[3] INCAS – National Institute for Aerospace Research "Elie Carafoli",
B-dul Iuliu Maniu 220, 061126 Bucharest, Romania
radub@incas.ro

Key words: CFD, Self-starting performance, Counter-rotating VAWT, Renewable energy.

Abstract. This research is focused on computational investigation on unsteady flow with various turbulence intensities, around of a three-blade H-rotor wind turbine (the conventional VAWT configuration). The study is also dedicated to investigate the causes that lead to the inability of the VAWT turbines with fixed pitch and low solidity to self-start with the aim of identifying solutions to overcome them. The consideration of starting behavior, therefore, offers a supplementary solution to improve the overall performance. In the second part of this work, a two counter rotating rotors configuration is numerically investigated to determine the efficiency and to fully understand the flow physics structure around it. For this analysis, URANS and LES CFD methods are used, with the proper choice of the turbulence model. Based on the preliminary numerical results, it is estimated that this new unconventional configuration will have greater efficiency, approximately 8% more, compared to a standard VAWT configuration.

1 INTRODUCTION

In urban or offshore areas the wind is fluctuating and unstable with fast changes in direction and intensity. In these environments the use of small vertical axis wind turbines (VAWT) is preferred due to several advantages over horizontal axis wind turbines (HAWT), at least after more thorough studies on the possibility of self-start at relatively low speeds or low Reynolds numbers [1]. The research in small-scale VAWT, with a rotor diameter of only several meters, is motivated by the future demand for a decentralized and sustainable energy supply in urban and rural environment. VAWT can work for all wind directions and it

requires low wind speed (2 m/s) [2]. However, the VAWT has lower rotational speed and efficiency than HAWT in which a maximum tip speed is not over double of wind speed and 17 –30 % of efficiency [3]. Nevertheless, the efficiency of VAWT will be increased by adding some equipment, such as Savonius type of main turbine, resulting in reducing of the cut in wind speed [4] or by using an unconventional configuration, composed on two co-axis counter-rotating rotors.

The rotor configuration composed of a number of blades with a chord to diameter ratio and blade aspect ratio, implies the azimuth variation of the bound circulation of the blade, with an inherently unsteady regime operation. Both the vorticity structure and the velocity/pressure field around the blade, resulting in a complicated wake composed mainly of shed vorticity, change depending on the operation regime. As the operation of VAWT implies the occurrence of all tip speed ratios (TSR) from the start-up regime up to the operating condition, a better understanding of the wake-flow physics and the blade-wake interaction in off-design operations is need in order to achieve self-starting machines appropriate to the urban applications.

This research is focused on computational investigation on a dynamic stall phenomenon associated with unsteady flow around straight three-blades H-rotor (the standard H-VAWT configuration, Fig. 1a).

Numerical simulations take into account the wind regime at various turbulence intensities to determine possible influences on the self-starting stage and turbine performance. Finally, a proper combination of geometric and flow parameters could be determined, suitable both for a self-starting regime at low speeds and for a good efficiency at average wind speeds.

The combination of two vertical axis wind turbines was studied by many researches with the task to improve the starting phase [5]. In the second section of this work a two counter rotating rotors configuration (CR-VAWT), Figure 1b, was numerical investigated in order to determine the efficiency and to understand the flow physics structure around it.

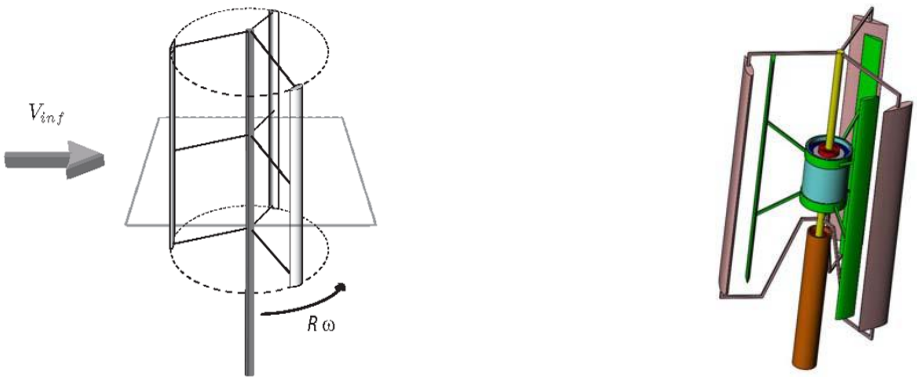

a) b)

Figure 1: a) Standard straight blade VAWT; b) Co-axis counter rotating VAWT

For this analysis, URANS and LES CFD methods will be used, with the proper choice of the turbulence model. Based on the preliminary numerical results, it is estimated that this new unconventional configuration will have a greater efficiency, approximately 8% more, compared to a standard VAWT configuration.

2 TURBULENCE INTENSITY EFFECTS ON A STANDARD VAWT EFFICIENCY

The flow through a VAWT rotor is entirely unsteady and is dictated by the dynamic stall [6,7] and turbulence intensity of the wind.

The turbulence intensity *I* is defined by the ratio of the vector norm of the fluctuating part (u') and the average of the mean velocity (*U*):

$$I = u'/U \tag{1}$$

$$u' = \left[\left(u_x'^2 + u_y'^2 + u_z'^2\right)/3\right]^{1/2} \tag{2}$$

$$U = \left[\left(\bar{u}_x^2 + \bar{u}_y^2 + \bar{u}_z^2\right)/3\right]^{1/2} \tag{3}$$

The overall objective of this study is to investigate how the performance of a standard VAWT is influenced by the different turbulence intensity degree of the incoming flow field. Results are presented in terms of power coefficients, quantifying the performance parameters with varying inflow conditions. In real life (wind turbines on the roof in urban environment or for offshore wind turbines) the wind turbine operates in the atmospheric boundary layer, which typically has a turbulence intensity of order of 10 to 25 %

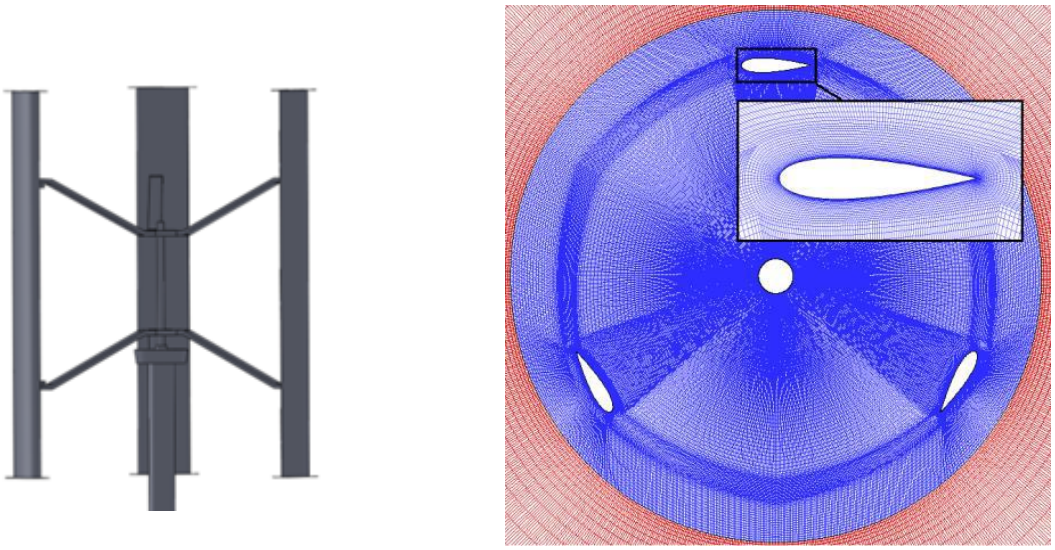

Figure 2: The 2D mesh for the standard VAWT

2.1 Numerical methods

For numerical investigation of the flow around a VAWT, commercial CFD codes using standard methods URANS or LES models can analyze both the unsteady flow and turbulence effects [9]. If in the past URANS models were inaccurate in the transition zone between laminar and the turbulent regime a new developed model, adopted to the standard SST model, having four transport equations, can also capture transition [10].

In Fig.2 is shown the two-dimensional computational meshes used for the stationary domain and the rotating domain that includes the blades.

This turbine is designed to generate up to 5.5 kW power at a wind speed of 8 m/s. Table 1 shows the geometric parameters of the entire system. For the actual airfoil the NACA 0021 was chosen which has a well behavior even at post-stall angles of attack.

Table 1: The geometric wind turbine charateristics

Parameter		Value
Rotor diameter	D [m]	3.6
Height rotor	h [m]	4.5
Number of blades	N	3
Height of whole wind turbine	H [m]	16
Blade chord	c [m]	0.6

The computational domain was divided into two subdomains. One that is rotating - containing the blades and the shaft of the wind turbine, and one is stationary - representing the far field. Figure 2 presents the structured mesh created for this set of numerical experiments.

For this analysis, an Unsteady Reynolds Averaged Navier-Stokes (URANS) model was used to study the effects of turbulence intensity on the efficiency of the wind turbine. Thus we chose different values of intensity on the far field boundary of the computational domain, this is seen a replacement for the practical case where a turbulence inducing grid or obstacle would typical influence the flow upstream. Turbulence intensity values were considered at multiple values between 1% and 20%. The URANS models were used in conjunction with the SIMPLE pressure-velocity coupling method. All tests were performed in 2D case with the corrected transition SST turbulence model.

Since the flow at the starting regime is the one of interest in this paper, and that it is characterized by low Reynolds numbers, the adapted transition SST model was used to account for boundary layer transition. Detailed formulation of a model of turbulence can be found in the work of Menter et al. [11] and Langtry et al [12].

Menter's Transition SST turbulence model was first detailed in [10] and it is a model with four equations. In the standard equations of *k*-ω SST model a further two equations are meant to solve problems that arise in the transition zone between the laminar and turbulent region.

The transport equation for the kinetic turbulent energy, *k*, is written as follow:

$$\frac{\partial k}{\partial t}+\bar{u}\frac{\partial k}{\partial x}+\bar{v}\frac{\partial k}{\partial y}+\bar{w}\frac{\partial k}{\partial z}= \tag{4}$$
$$=\frac{1}{\rho}\left[\frac{\partial}{\partial x}\left(\Gamma_k\frac{\partial k}{\partial x}\right)+\frac{\partial}{\partial y}\left(\Gamma_k\frac{\partial k}{\partial y}\right)+\frac{\partial}{\partial z}\left(\Gamma_k\frac{\partial k}{\partial z}\right)\right]+\tilde{G}_k-Y_k\,.$$

The transport equation of the specific rate of dissipation (ω):

$$\frac{\partial \omega}{\partial t}+\bar{u}\frac{\partial \omega}{\partial x}+\bar{v}\frac{\partial \omega}{\partial y}+\bar{w}\frac{\partial \omega}{\partial z}= \tag{5}$$
$$=\frac{1}{\rho}\left[\frac{\partial}{\partial x}\left(\Gamma_\omega\frac{\partial \omega}{\partial x}\right)+\frac{\partial}{\partial y}\left(\Gamma_\omega\frac{\partial \omega}{\partial y}\right)+\frac{\partial}{\partial z}\left(\Gamma_\omega\frac{\partial \omega}{\partial z}\right)\right]+G_\omega-Y_\omega+D_\omega\,.$$

where, Γ_k, and Γ_ω are the terms that represent the effective diffusivities of k, and ω, respectively; D_ω is the positive part of the cross-diffusion term; $\tilde{G}_k$ represents the production of turbulence energy; G_ω represents the production of ω.

$$\Gamma_k = \mu + \frac{\mu_t}{\sigma_k}, \Gamma_\omega = \mu + \frac{\mu_t}{\sigma_\omega}. \tag{6}$$

The second methods, LES [13], involve the filtering of the Navier-Stokes equation.

2.2 Results and discussions

The results of the flow simulations confirm that the flow is in transition on a significant chord length of the airfoil used for the wind turbine blades, therefore the use of the additional two transport equations of the model is justified.

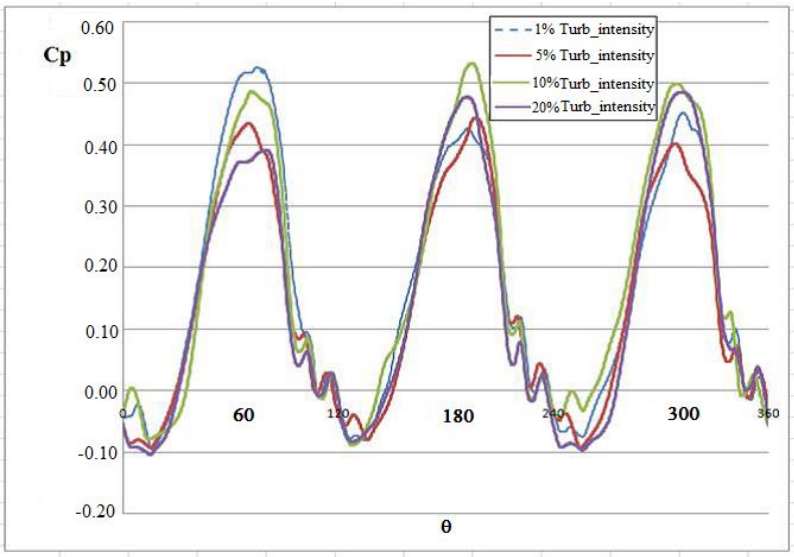

Figure 3: The power coefficient variations with turbulence intensity

In determining the influence of turbulence intensity on the efficiency of a standard VAWT at the starting phase, in Figure 3 the power coefficient variations on a full rotation for the investigated cases is plotted.

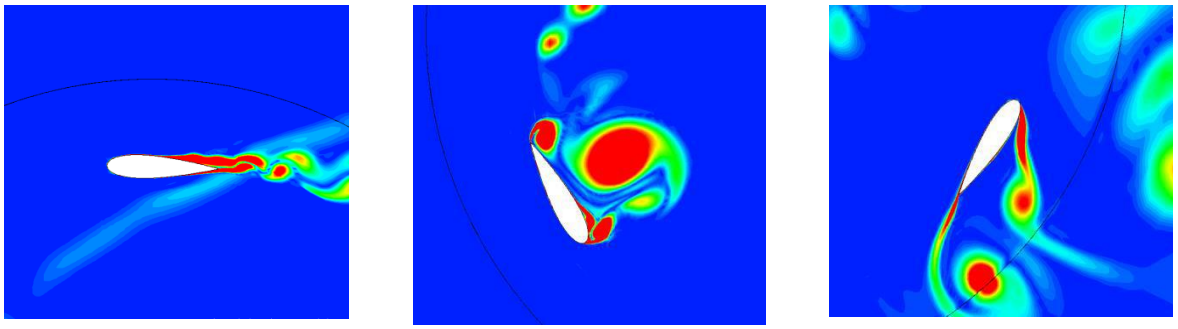

a) b) c)

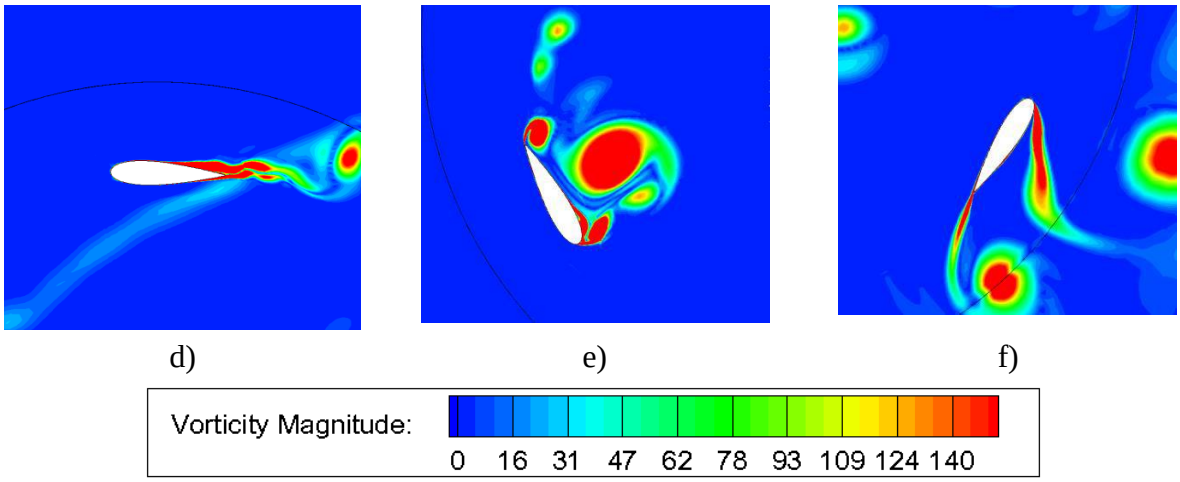

Figure 4: The vorticity magnitude for :
a) 0degree position and 5% turbulence intensity; b)120degree position and 5% turbulence intensity;
c) 240degree position and 5% turbulence intensity;
d) 0degree position and 20% turbulence intensity; e)120degree position and 10% turbulence intensity;
f) 240 degree position and 20% turbulence intensity

In Figure 4 is shown the variations of vorticity magnitude for various positions of the wind turbine blades. Thus variations are provided for azimuth positions of 0°, 120° and 240° and for the turbulent intensity values of 1%, 5%, 10% and 20% (only for 5% and 20% represented here).

Moreover, on average, the maximum power coefficient is highest when the turbulence intensity is at about 10%. In addition to this, the variation of the Cp with azimuth angle also displays an oscillation of much lower amplitude and frequency.

3 NUMERICAL ANALYSIS FOR CO-AXIS COUNTER-ROTATING VAWT

The combination of two VAWTs was studied by many researchers [3]. The usual combination is between Darrieus and Savonius types [5-6]. This configuration, Darrieus-Savonius was used to improve Darrieus wind turbine starting phase. It is well known that the Savonius rotor creates high torque and is self-starting even at low wind speed, but is relatively

Table 2: The geometric parameters of the CR-VAWT

Parameters	Value		Units
	Turbine_in	Turbine_out	
Airfoil	NACA 0021	NACA 0021	-
Blade chord	0.3	0.5	m
Turbine diameter	1.8	2.4	m
Turbine height	3.6	3.6	m
Number of blades	3	3	-
Design velocity	10		m/s
Design power	2000		W

low in efficiency rating. The Darrieus rotor is not a self-starting rotor, but has much higher

efficiency than the Savonius rotor. The combination of rotors increase the total power of the turbine in lower wind speed [9].

In this section a new-concept of counter-rotating rotors are analysed. The co-axis CR-VAWT have two H-type rotors with three blades each, designed using the NACA 0021 airfoil.

In the Table 2 the geometric characteristics of this wind turbine are presented.

3.1 Geometry and boundary conditions setup

For the numerical simulation a 2D domain has been defined. The domain was further split in four subdomains, two stationary and two rotating. The rotational subdomains contains the blades of the inner and outer turbine and the stationary subdomain are represented by the

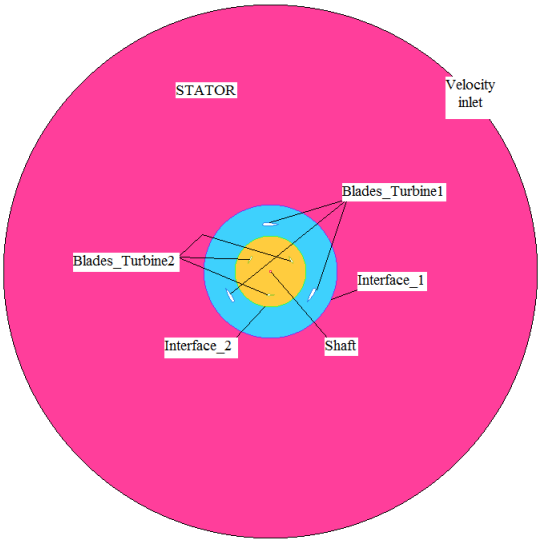

Figure 5: Computational domain for the CR-VAWT

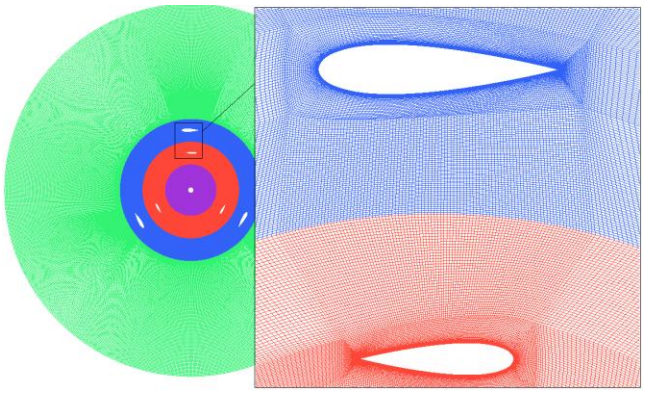

Figure 6: 2D Mesh of the wind turbine

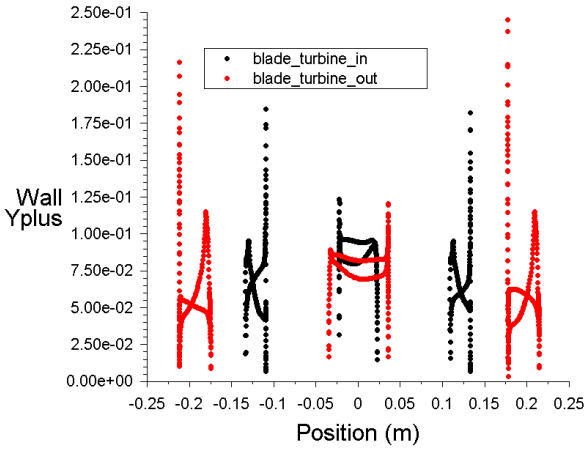

Figure 7: Blades y^+ value

environment around the wind turbine and from the inner domain which is also a stationary one. Figure 5 shows the computational domain with the four subdomains.

The grid was generated using the ICEM CFD software, by using the blocking function, in order to have a structured grid with hexa-elements. To resolve the flow from boundary layer, the y^+ value has been set lower than 1, and the growth ratio of the elements was set to 1.05. Figures 6 and 7 show the grid and the value of y^+, starting from the leading edge, all the way to the trailing edge of the all six blades depending the their position.

The CFD numerical models work by solving the Navier-Stokes system of equations. To simulate the flow around the wind turbine, the commercial software ANSYS fluent has been used. Table **3** shows the required input parameters of a CFD case.

The CFD simulations of CR-VAWT rely on the mesh model, which works by selecting a set rotational speed for the rotor and performing several studies in order to determine the nominal point of the turbine.

To understand the flow physics around CR-VAWT, the time-dependent characteristics of the simulation, the Unsteady Reynolds Averaged Navier-Stokes based on turbulence model SST, was employed in this study, because of its successful history of accurately predicting the performance of wind turbines.

Table 3: Ansys Fluent case setup

Models	Solver	Pressure Based	Unsteady	2D
	Viscous Model	k-ω SST		
Materials	Air	Density, constant		
Operating conditions	Pressure 101325[Pa]			
Boundary Condition	Inlet	Velocity inlet V_x=13m/s		
	Blades	wall		
	Shaft	wall		
	Interfaces	Interface rotor-stator and rotor-rotor		
	Rotors	Mesh motion		
	Stators	Stationary		
Solve	Controls	Solution	Courant nr = 5	Discretization 2^{nd} order upwind
	Initialize	Inlet, Velocity=13m/s		
	Monitors	Residuals	10^{-3}	
		Force	Momentum coefficient	
	Iterate	1800 Steps	0.001s time step size	
Report	Reference values	Inlet	Length = turbine radius	

3.2 Results and discussions

In Figure 8, torque coefficients, C_m, are presented for each rotor of the CR-VAWT, at two TSRs and in Figure 9 power coefficients, C_P, are presented for each rotor of the CR-VAWT.

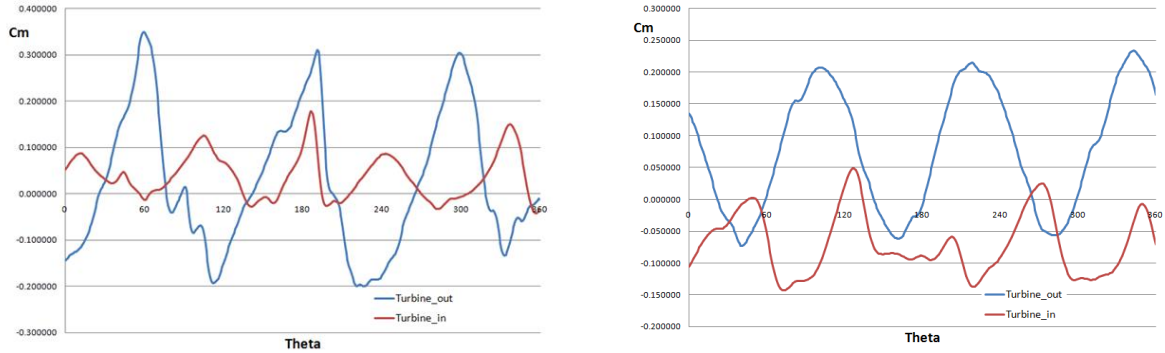

a. b.

Figure 8: 2D Torque coefficient C_m variations for each CR-VAWT rotor: a) TSR=1; b) TSR=3

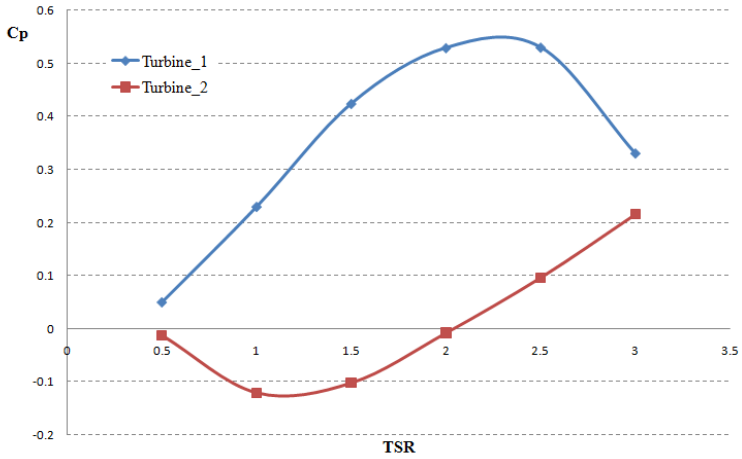

Figure 9: Power coefficients - $C_P(TSR)$ of a two co-axis rotors CR-VAWT

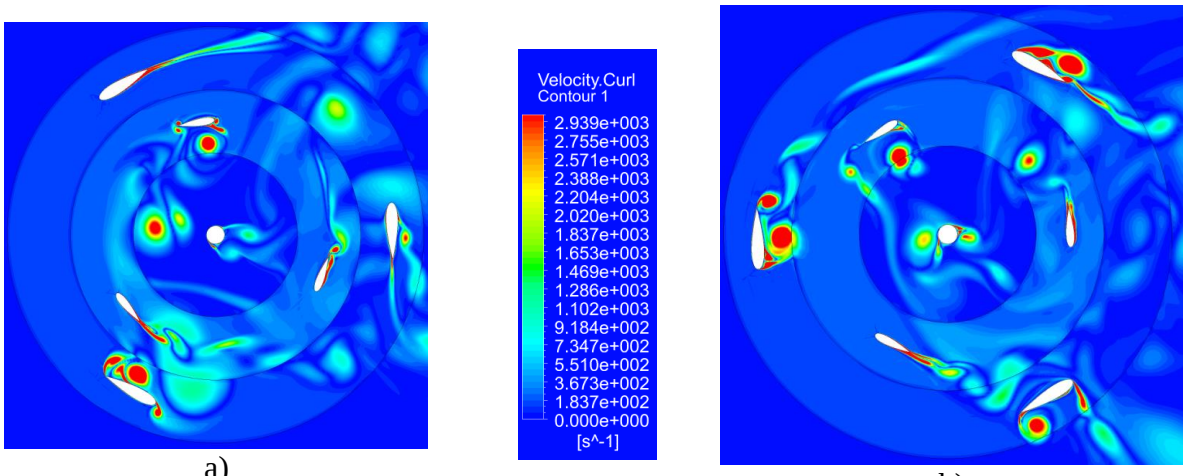

a) b)

Figure 10: Vorticity magnitude contours for TSR 1: a) $\theta = 30°$; b) $\theta = 90°$

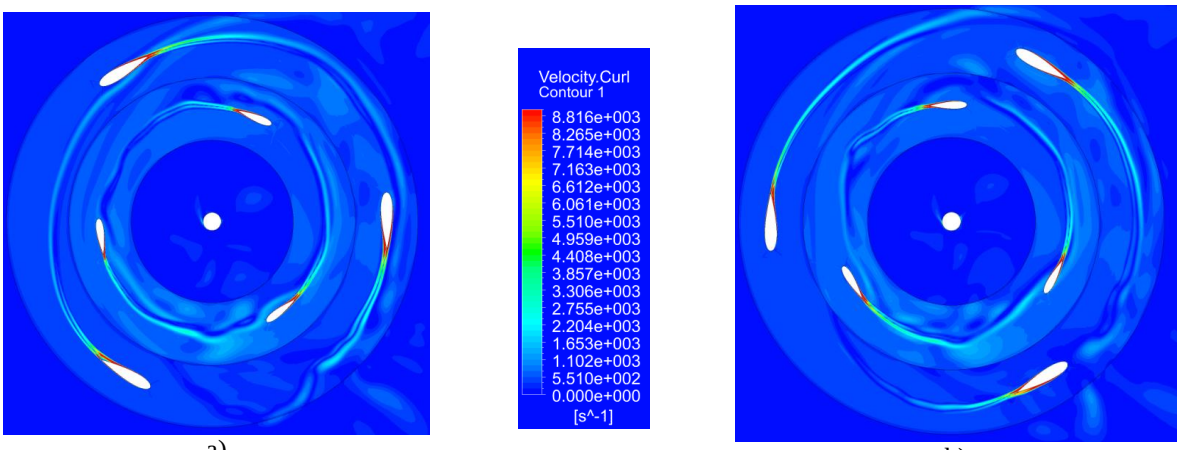

a) b)

Figure 11: Vorticity magnitude contours for TSR 3:a) $\theta = 30°$; b) $\theta = 90°$;

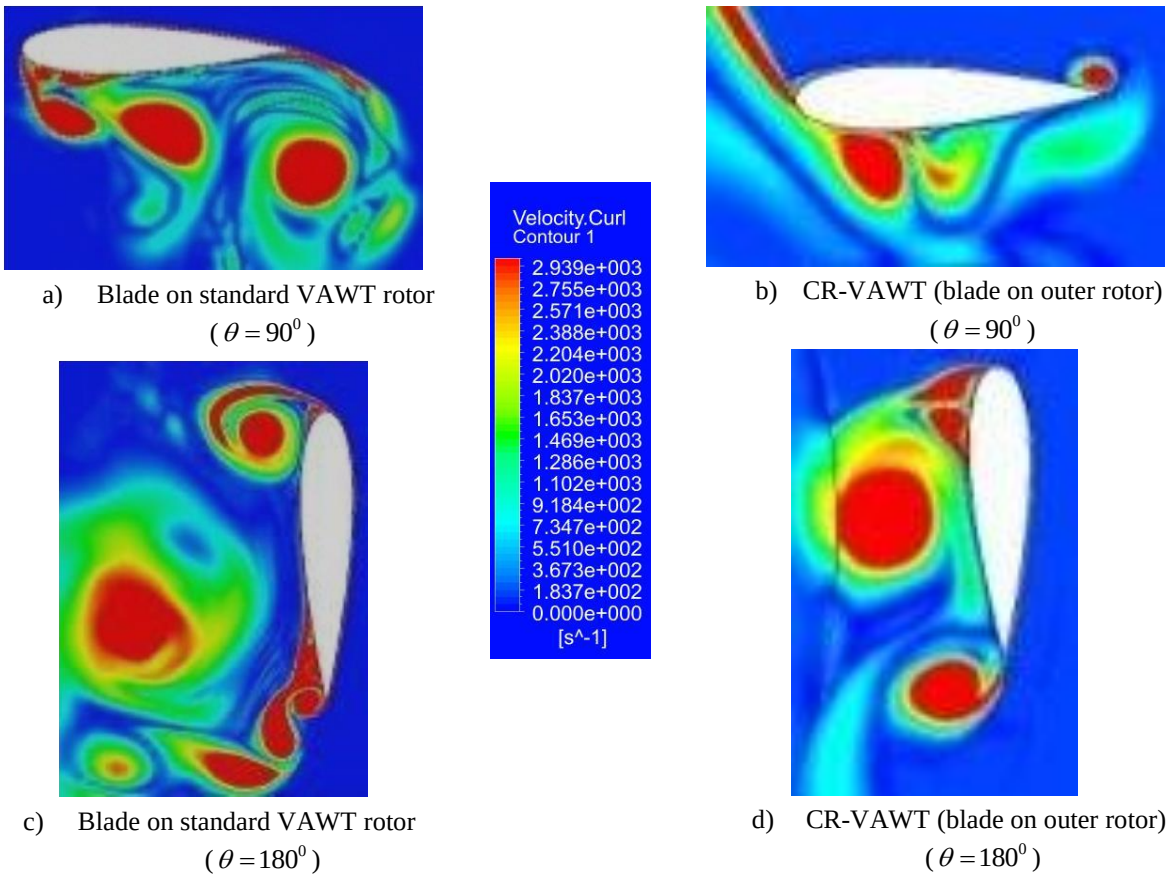

a) Blade on standard VAWT rotor ($\theta = 90^0$)

b) CR-VAWT (blade on outer rotor) ($\theta = 90^0$)

c) Blade on standard VAWT rotor ($\theta = 180^0$)

d) CR-VAWT (blade on outer rotor) ($\theta = 180^0$)

Figure 12: Comparative vorticity magnitude contours for TSR 1: a) and c) - blade on standard VAWT rotor; b) and d) - blade on outer rotor of CR-VAWT

Dynamic stall is an inherent effect of the operation of a VAWT at low tip speed ratios $(TSR \le 3)$ where for $TSR \sim 1$ the turbine starting behavior is crucial for the rotor enters its steady operating state. At low speed ratios, in the range of chord Reynolds number

$\mathrm{Re} = 10^5 - 10^6$, the near wake is captured inside the rotor and its shed vorticity is accumulated and concentrated at the windward quarter ($0^0 < \theta \le 90^0$) of the rotation. Then in the leeward quarter ($90^0 < \theta \le 180^0$) of the rotation, the concentrated more and less vortical structures detach from the airfoil (centrifugal effect) and these induce a velocity/pressure field around airfoil resulting in the change of aerodynamic forces, i.e. the significant drag reduction. This is the drag dynamic stall event promoting the continuous thrust-producing and self-starting [1]. Figure 12 illustrates comparatively the dispersion of the clockwise vorticity shed after the roll-up of leading-edge ($TSR = 1.0, \mathrm{Re} = 10^5$) for the conventional 3 blade rotor and a 3 blade contra-rotating rotors. For this comparison, the results were obtained by numerical investigation of a conventional VAWT with the same rotor as the outer rotor of the CR-VAWT. It is observed that there are differences in the evolution of the clockwise vorticity shed from airfoil after its rolling, which implies that the contra-rotating rotor is a solution capable of making the VAWTs to self-start, Figures 10 and 12.

At high tip speed ratio ($TSR > 3$) the two velocity fields are uncoupled and the outer rotor is running without compromising the wind turbine performance, Figure 11.. But more the twisted flow between rotors has a beneficial effect on the general operating of the main/outer rotor, a power gain of 8 % is estimated.

4 CONCLUSIONS

In the first part of the paper, the overall objective of this study was to investigate how the performance of a standard VAWT is influenced by the different turbulence intensity degree of the incoming flow field. Results are presented in terms of power coefficients, quantifying the performance parameters with varying inflow conditions.

- A moderate turbulence intensity have a beneficial influence on the VAWT performance, but a high degree of turbulence has several negative impacts on wind turbines.
- On average, the maximum power coefficient is highest when the turbulence intensity is at about 10%. In addition to this, the variation of the Cp with azimuth angle also displays an oscillation of much lower amplitude and frequency.

In the second part of the paper, the work focuses on the numerical analysis of the behavior of the flow around a CR-VAWT capable to self-start. The analysis and their CFD computational results lead to the following conclusions:

- The airfoil in Darrieus motion at $TSR \sim 1$, in the range of $\mathrm{Re} = 10^5 - 10^6$ generates concentrated vorticity shed that can be exploited to induce aerodynamic forces capable of making the wind turbines self-start.
- The Darrieus turbine operates with two distinct modes during start-up: continuous lift-driven mode along the windward quarter of the rotation and discrete lift-drag driven mode along the leeward quarter of the rotation.
- The ability to escape from the dead-band is directly related to the evolution of clockwise vorticity shed where the concentration of vorticity intensified in the flow field of contra-rotating rotor regularizes the discrete operating mode.
- At high tip speed the twisted flow field between rotors improves the general operating of the turbine increasing its efficiency.

- The significantly improved exploitation of the contra-rotating concept applied to VAWTs based on the drag dynamic stall and twisted flow effects can be achieved by properly sizing the contra-rotating rotor configuration.

REFERENCES

[1] H. Dumitrescu H., Cardos V., Malael I., The physics of starting process for vertical axis wind turbines, in Chap. 7, E. Ferrer and A. Montlaur (eds.), *CFD for Wind and Tidal Offshore Turbines*, Springer Tracts in Mech. Engng., pp. 69-81, (2015).

[2] Manwell J.F., McGowan J.G. and Rogers A.L. (2002). *Wind Energy Explained*: John Wiley & Sons; Baffins Lane, Chic Hester, West Sussex PO19 1UD, England.

[3] Menet J.-L., A double-step Savonius rotor for local production of electricity: a design study. *Renewable Energy*, (2004) **29**:1843–1862.

[4] Jack Park. (1975). *Simplified Wind Power System for Experimenters.* 2nd edition: Helion.

[5] Gavaldà Jna. Massons J., Díaz. F., Experimental study on a self-adapting Darrieus — Savonius wind machine, *Solar & Wind Technology,* (1990), **7:**457-461.

[6] Tjiua W., Marnotob T., Mata S., Ruslana M. H., Sopiana K., Darrieus vertical axis wind turbine for power generation II: Challenges in HAWT and the opportunity of multi-megawatt Darrieus VAWT development, *Renewable Energy*, (2015) **75:** 560–571.

[7] L. A. Danaoa, J. Edwardsb, O. Eboibic, R. Howellc, A numerical investigation into the influence of unsteady wind on the performance and aerodynamics of a vertical axis wind turbine, *Applied Energy*, (2014) **116**: 111–124.

[8] Geernaert G. L., Larsen S. E., Hansen F., Measurements of the wind stress, heat flux, and turbulence intensity during storm conditions over the North Sea**,** *Journal of Geophysical Research: Oceans*, (1987), **92:** 13127-13139.

[9] Mălăel I., Drăgan V., Vizitiu G., The vertical axis wind turbine efficiency evaluation by using the cfd methods, *Applied Mechanics and Materials*, (2015) 772: 90-95.

[10] Menter F. R., Esch, T. and Kubacki, S., Transition Modelling Based on Local Variables, *5th International Symposium on Turbulence Modeling and Measurements*, Spain, 2002.

[11] Menter F., Ferreira T., Esch B., Konno B., The SST Turbulence Model with Improved Wall Treatment for Heat Transfer Predictions in Gas Turbines, *Proceedings of the International Gas Turbine*, Congress 2003 Tokyo, November 2-7, 2003.

[12] Langtry R.B., Menter F.R., Transition Modeling for General CFD Applications in Aeronautics, AIAA 2005-522.

[13] Franke J., Hellsten A., Sclunzen H., Carissimo B., Best practice for the CFD Simulation of Flows in the Urban Environment: *COST Action 732 Quality Assurance and Improvement of Microscale Meteorological Models*, 2007: Meteorological Inst.